Quantum Effects of Phase Transitions in Ferroelectric Crystals -- Experiments and Models --

Hiroyuki MASHIYAMA, Serges E. MKAM TCHOUOBIAP and Tatsuki MIYOSHI
Department of Physics, Faculty of Science, Yamaguchi University,
Yamaguchi 753-8512, Japan

(Accepted: June 19, 2008)

From structural data obtained experimentally, some microscopic parameters can be estimated unambiguously. By using these parameters, a quantum Ising model can explain the isotope effect in $SrTiO_3$ and KH_2PO_4. The ferroelectric transition in ^{18}O isotope crystal of $SrTiO_3$ is successfully explained only by a mass effect in quantum state, which demonstrates importance of quantum effects in ferroelectrics.

Keywords isotope effect, $SrTiO_3$, KH_2PO_4, structure parameters, quantum Ising model, quasi-harmonic model, quantum paraelectricity, Barrett's relation, phase diagram

Introduction

So far as a phase transition takes place at room temperature, classical thermodynamics account the physical properties successfully. However, KH_2PO_4 (KDP) has been considered to be a quantum system [1], because proton is light enough to display the quantum behavior around the phase transition temperature of 123K [2]. Therefore a quantum Ising model (QIM) has been applied to explain the remarkable isotope effect between proton and deuteron [1,3-5]. Another example of the quantum system is $SrTiO_3$ (STO), in which the quantum fluctuation (zero-point vibration) is considered to destroy the ferroelectric order even at zero temperature [6]. The quantum paraelectric character of STO is demonstrated by Barrett's relation of the permittivity [7,8].

About a decade ago, ferroelectricity was discovered in STO18, where oxygen of STO is replaced by a heavy isotope ^{18}O [9]. The transition temperature (T_c) decreases with reducing the ^{18}O concentration x [9,10]. The temperature dependence of the permittivity for the mixed crystal $SrTi^{16}O_{1-x}{}^{18}O_x$ (STO-x) was successfully fitted to the Barrett's relation [10]. The phase transition has been explained by using three-state quantum Ising model [11]. The T_c-x phase diagram can also be explained by a quasi-harmonic model (QHM), if the effective mass of STO is assumed, and interactions depend on x, properly [12].

Although the Barrett's relation was introduced firstly in STO where the transition was considered as displacive type, the same relation was used in KDP under hydrostatic pressure (p) [13]. The T_c-p phase diagrams of KDP and deuterated KDP can be explained also by QHM [14], as well as by QIM [15]. Because a theoretical calculation is very sensitive to the model parameters, proper values should be determined by using experimental results, as reasonable as possible.

In this report we display how to estimate the microscopic parameters from experimental results. By using quantum models with these reasonable parameters, we can explain the isotope effect in STO and KDP.

Formulation

Let us consider an atom with an effective mass m located within the self-potential $V(x)$. We assume a bilinear interaction between the adjacent cells. The mean-field Hamiltonian is written by

$$H = \frac{p^2}{2m} + V(x) - (\gamma\xi + h)x \quad , \tag{1}$$

where $\xi = \langle x \rangle$, γ and h are the order parameter, the interaction parameter and applied field, respectively. Once quantum states in the self-potential are solved, the free energy, entropy, specific heat and permittivity are obtained by the linear response theory [16]. If the phase transition takes at low enough temperature, only two quantum states would be decisive for the thermodynamic quantities; this is a QIM limit. Another tractable method is to replace $V(x)$ by an effective harmonic potential; QHM. It has been noted that both QIM and QHM give the Barrett's relation for susceptibility χ: [11]

$$\chi = \frac{{x_0}^2 / k_B}{\frac{T_1}{2}\coth\left(\frac{T_1}{2T}\right) - T_0} \quad , \quad T > T_c \quad . \tag{2}$$

Here T_1 is the energy gap between the two quantum states and T_0 is the interaction energy given by

$$T_0 = \gamma {x_0}^2 / k_B , \tag{3}$$

where $x_0 = \langle 0 | x | 1 \rangle$ in QIM, or $\hbar T_0 = \langle x^2 \rangle_{T=T_c} mk_B T_1^2$ in QHM. In both models, T_0 increases with the interaction parameter γ.

The transition temperature T_c is given by a common equation for the both models as

$$T_c = T_1 \Big/ \ln\left(\frac{2T_0 + T_1}{2T_0 - T_1}\right) . \tag{4}$$

In a classical limit $T_0 >> T_1$, $T_c = T_0$. However, T_c decreases logarithmically with increasing T_1/T_0, and vanishes for $T_1>2T_0$. The quantum fluctuation surpasses the interaction energy, and ferroelectric order does not appear down to 0 K.

Hereafter we assume that the self-potential $V(x)$ is given concretely by

$$V(x) = 2D\exp(-ad)\{\exp(-ad)\cosh(2ax) - 2\cosh(ax)\}. \quad (5)$$

The parameter d represents the splitting distance of two Morse potentials located back-to-back. The quantum states |0> and |1> are calculated as a function D/m, a and d, by solving the Schrödinger equation numerically. Physical quantities are calculated straightforwardly by using quantum thermodynamics as reported previously [17].

Parameters for STO

First we mention how the self-potential parameters can be estimated from the Debye-Waller factors of STO reported by Jauch and Palmer [18]. If the stretching motion of Ti-O is hard, then we can put d=0 in (5) and approximate as $V \cong -2D + 2Da^2x^2$. For the ground state of the parabolic potential, the expected value is $< x^2 >= \hbar/4a\sqrt{mD}$, which should coincide with $U_{//} = 0.00222$ A^2; the Debye-Waller factor of O at 111K in the cubic phase. Generally speaking, we can expect that the harmonic frequency $\nu = a/\pi \cdot \sqrt{D/m}$ is order of 15-30 THz (500-1000cm^{-1}). Therefore, one of the plausible set of parameters is m=16 in atomic mass unit, D=0.2 eV and a=4 A^{-1}, for which the single molecular frequency is 15 THz.

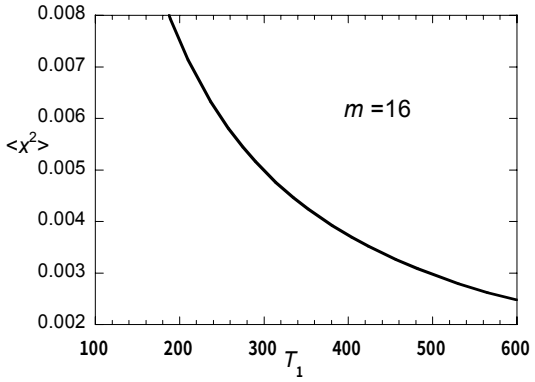

Figure 1 The relation between <x^2> and T_1 for m=16.

The paraelectric-ferroelectric transition would be referred to the Slater-mode: the bending motion of Ti-O-Ti. The restoring force for O works from Ti as well as distant Sr and other O's. The self-potential may be given by (5) with finite d. The calculated relation between <x^2> and

T_1 is plotted in Fig. 1 for m=16. The curve is almost universal for any Da^2 and d, so far as the ground-state wave function is single-peaked.

The Debye-Waller factor at 50K has been reported as $U_{11} = 0.0057\,\mathrm{A}^2$ [18], and the Barrett's parameter T_1 ~84K [9]. In order to explain these facts, we have to take the effective mass of the Slater mode is 50~70, because the quantum energy in the Schrödinger equation can be scaled by the mass. Here we assume that half of the Debye-Waller factor U_{11} comes from the acoustic phonon and the rest from the Slater mode, and two units of STO are coupled to induce the ferroelectric structure. Then the effective mass m will be given by the following,

$$\frac{1}{m} = \frac{1}{2(M_{\mathrm{Sr}} + M_{\mathrm{Ti}})} + \frac{1}{6M_{\mathrm{O}}} \quad , \tag{6}$$

where M_{Sr}, M_{Ti} and M_{O} represent the respective atomic mass. Further the oxygen mass is considered to be given by the mean mass of $(1\text{-}x)^{16}$O and x^{18}O. The interaction may be magnified by six in comparing with a single O case.

Figure 2 shows the calculated transition temperature T_c given by (4) with parameters D=1.2eV, a=4A^{-1}, d=0.18A and γ=1.39eV/A^2. The interaction parameter γ is adjusted in order to give the critical replacement ratio as x_c=0.329. Here x=0 (m=70.87) and x=1 (m=77.60) are STO16 and STO18, respectively.

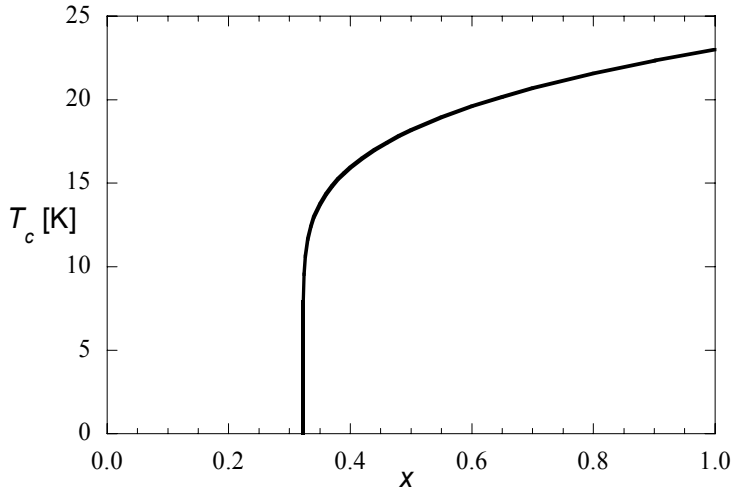

Figure 2 The transition temperature T_c against the replace ratio x of ^{16}O by ^{18}O in $SrTiO_3$. The effective masses 70.87 and 77.60 are for x=0 and 1, respectively.

We can choose other set of parameters, for example, D=0.2eV, a=4A^{-1}, d=0.18A, γ=0.613eV/A^2 and m=48~54. Additional assumption of x-dependent parameters may give better agreement between the calculated and observed phase diagram T_c-x, but let us settle the above parameters.

Susceptibility and soft mode of STO

The paraelectric susceptibility is given by the Barrett's relation (2). The similar formula for the ferroelectric susceptibility can be given analytically. The temperature dependence is demonstrated in Fig. 3(a) for $x>x_c$ and (b) for $x<x_c$. At high temperature (T > 50 K), the susceptibility χ obeys to the classical Curie-Weiss law, however, the quantum fluctuation suppress the transition temperature a little. For $x<x_c$, χ keeps a large plateau at low temperature.

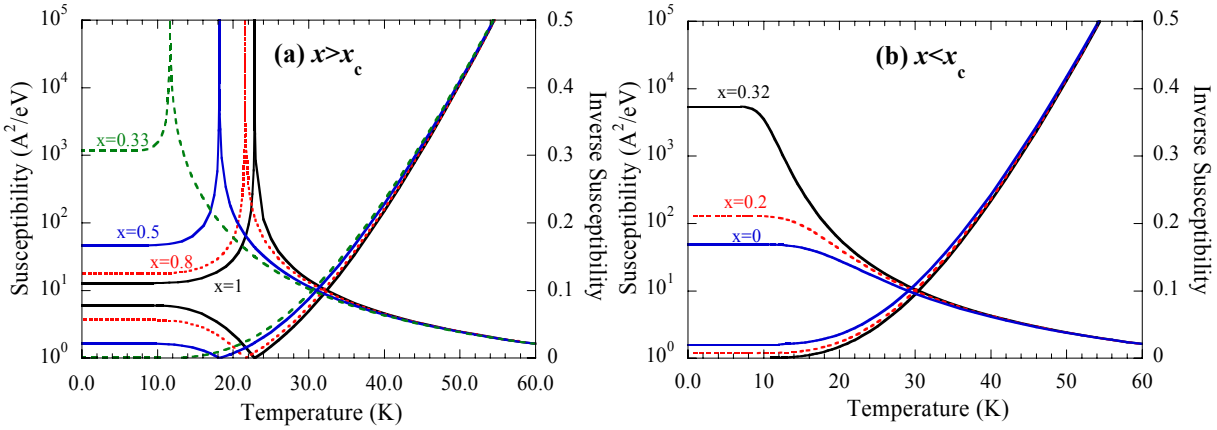

Figure 3 Temperature dependence of susceptibility and the inversed one.

The soft mode frequency can be expressed by an analytical relation both above and below T_c [19]. The temperature dependence of the soft mode is plotted in Fig. 4. Although the frequency decreases $(T\text{-}T_c)^{1/2}$ just near the transition temperature, the temperature dependence becomes rather linear in the quantum regime. In the ferroelectric phase the soft mode frequency is proportional to the order parameter ξ. The calculated frequencies for STO18 are 38 cm^{-1} at 60K and 16 cm^{-1} at 0K; the former is in agreement with the observed one 3-4meV; 24-32cm^{-1} [11], and the latter is consistent with 13 cm^{-1} [20]. Our theory supports the complete softening of the phonon mode observed in the Raman spectrum [20].

Parameters for KDP

We have determined the structural change of KDP through the ferroelectric 123K transition by using neutron scattering data [21]. Proton density is obtained by maximum entropy method. The density distribution can be characterized by three parameters $U_{xx}=\langle x^2\rangle$, $U_{yy}=\langle y^2\rangle$ and $U_{zz}=\langle z^2\rangle$ in the paraelectric phase. Through the transition point, U_{yy} remains almost constant, however, U_{xx}=0.0453A^2 at 125K becomes 0.0173A^2 at 115K. From these values, we can guess the parameters in (5) for proton as D=2 eV, d=0.30A or D=4 eV, d=0.29A, and a=4A^{-1},

which are consistent with the previous ones. Therefore QIM can explain the *T*-*p* phase diagram of KDP as well as the isotope effect [15].

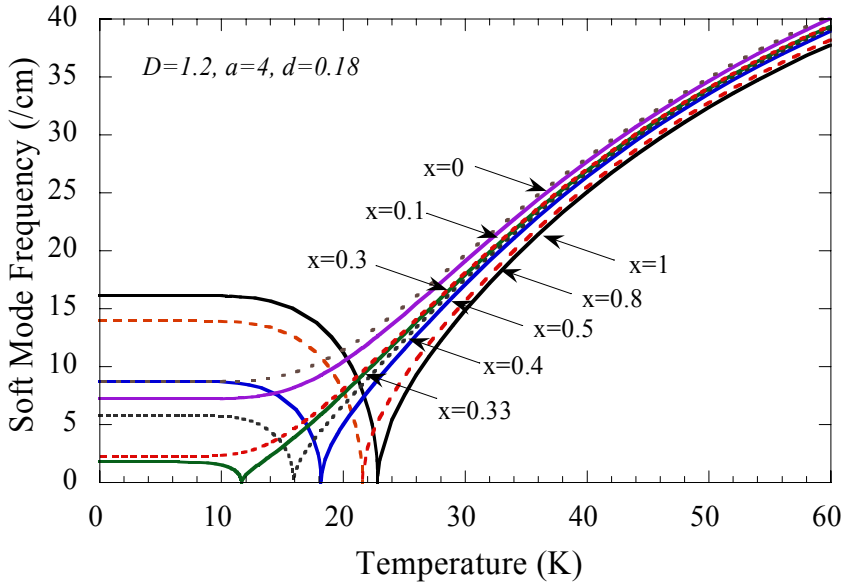

Figure 4 Calculated temperature dependence of the soft mode for STO-*x*.

Remarks

First we discuss about the crystal structure of KDP just above T_c. According to the refined analysis [21], only proton is in disorder and the PO_4 tetrahedron keeps a regular shape; it is not a disordered unit in the paraelectric phase. Once a proton attaches one side of oxygen below T_c, the PO_4 tetrahedron distorts to produce a dipole moment perpendicular to the O-H-O bond. Therefore two models can be accepted; (i) proton ordering is the trigger of the phase transition [15], or (ii) softening of the vibration mode of H_2PO_4 takes place at the transition [14].

Since the transition is at very low temperature in STO, ground and first excited states should be essential. This will be the reason why the T_c-*x* phase diagram of STO can be reproduced by either QIM or QHM [12]. The satisfactory results with QIM indicates that the quantum mass effect is essential in such phenomena as quantum paraelectricity, appearance of ferroelectricity with replacing heavy isotope or other kind of heavier atom, stress induced ferroelectricity, and so on.

Here let's comment on the isotope effect about Sr and Ti in STO. The natural masses are 87.62 and 47.867 for Sr and Ti, respectively. The scattering of the isotope is $^{84}Sr \sim {}^{88}Sr$ or $^{46}Ti \sim {}^{50}Ti$. The introduction of heavier isotope will rise the transition temperature 0.4K for $^{88}Sr^{50}Ti^{18}O_3$, if we follow the reduced mass equation (8). Such an effect is so small that

$^{88}Sr^{50}Ti^{16}O_3$ will keep paraelectric down to 0K. On the other hand, the critical replacing ratio x_c is expected to be 0.41 for $^{86}Sr^{46}TiO_3$. Such an isotope effect is not large but may smear the transition point, if the crystal is not homogenous in atomic mass.

Finally, our result is not sensitive to the self-potential form. The double Morse potential (5) may be replaced by quartic form $V(x)=ax^4+bx^2$, for which the oxygen isotope effect in STO could be explained only by the quantum mechanical mass effect [22].

References

[1] R. Blinc, J. Phys. Chem. Solids **13**, 204 (1960).
[2] J. Pirenne, Helv. Phys. Acta **22**, 479 (1949).
[3] P. G. de Gennes, Solid State Commun. **1**, 132 (1963)
[4] M. Tokunaga and T. Matsubara, Prog. Theor. Phys. **35** (1966) 581.
[5] R. Blinc and B. Zeks, *Soft Modes in Ferroelectrics and Antiferroelectrics*, (North-Holand, Amsterdam, 1974) Chapt. 5.
[6] K. A. Muller and H. Burkard, Phys. Rev. B **19**, 3593 (1979).
[7] J. H. Barrett, Phys. Rev. **86**, 118 (1952).
[8] E. Sawaguchi, A. Kikuchi and Y. Kodera, J. Phys. Soc. Jpn. **17**, 1666 (1962).
[9] M. Itoh, R. Wang, Y. Inaguma, T. Yamaguchi, Y.-J. Shan and T. Nakamura, Phys. Rev. Lett. **82**, 3540 (1999).
[10] R. Wang and M. Itoh, Phys. Rev. B **64**, 174104 (2001).
[11] Y. Yamada, N. Todoroki and S. Miyashita, Phys. Rev. B **69**, 024103 (2004).
[12] S. E. Mkam Tchouobiap and H. Mashiyama, J. Phys. Condensed Matter **20**, 055223 (2008).
[13] S. Endo, K. Deguchi and M. Tokunaga, Phys. Rev. Lett. **88**, 35503 (2002).
[14] S. E. Mkam Tchouobiap and H. Mashiyama, Phys. Rev. **B76**, 014101 (2007).
[15] H. Mashiyama, J. Korean Phys. Soc. **46**, 63 (2005).
[16] R. Kubo, J. Phys. Soc. Jpn. **12**, 570 (1957).
[17] H. Mashiyama, J. Phys. Soc. Jpn. **73**, 3466 (2004).
[18] W. Jauch and A. Palmer, Phys. Rev. B **60**, 2961 (1999).
[19] M. Tokunaga, Prog. Theor. Phys. **36**, 857 (1966).
[20] M. Takesada, M. Itoh and T. Yagi, Phys. Rev. Lett. **96**, 227602 (2006).
[21] H. Mashiyama, T. Asahi, H. Kasano and T. Miyoshi, *Neutron Activity Report on Neutron Scattering Research: Exp. Rep.,* (ISSP Univ. Tokyo, Tokai, 2006) Vol.**14**, No.96.
[22] Detailed analysis of the quartic potential will be published in J. Phys. Soc. Jpn. **77**, No.8 (2008)